Journal of Sound and Vibration (2003) **259**(5), 1181–1198
doi:10.1006/jsvi.2002.5204, available online at http://www.idealibrary.com on IDEAL®

VIBRATION ATTENUATION VIA CONSTRAINED LAYER DAMPING AND DASHPOT ON A SPRING–MASS–PLATE SYSTEM

S.-C. YU[†] AND S.-C. HUANG[‡]

Department of Mechanical Engineering, National Taiwan University of Science and Technology, 43*, Keelung Road, Sec.* 4*, Taipei, Taiwan* 106*, ROC. E-mail: schuang@mail.ntust.edu.tw; D*8203008*@mail.ntust.edu.tw*

(*Received* 28 *November* 2001, *and in final form* 20 *May* 2002)

The vibrations and damping characteristics of an annular plate with constrained layer damping (CLD) treatment subject to a traveling spring–mass–damper (SMD) are investigated. The equations of the CLD-treated plate are first derived from the energy principle. These equations are simplified via the Donnell–Mushtari–Vlasov assumptions. The response equations are eventually uncoupled for each mode and are in terms of a single-degree-of-freedom (s.d.o.f.) linear oscillator with hysteretic damping. The receptance method follows to joint the plate and the SMD, and the resulting change of natural frequencies and damping ratios are investigated. Individual effects due to the inertia and the stiffness are illustrated as well. The results shows that the damping ratios resulted from the viscoelastic core are more significant than that from the viscous damper. In addition, there exists a best design on the thickness of the viscoelastic material core to have the maximum damping ratios. The results also show that the attachment of SMD bifurcated the plate's natural frequencies for every mode but $n = 0$. The bifurcation becomes more obvious with the rotational speed. These results provide useful information for vibration suppression in engineering design.

1. INTRODUCTION

Due to the increasing demand on efficiency and reliability in mechanical systems, the control on structural vibration has become an important subject in the field of mechanical engineering design. Both active and passive suppression techniques can be utilized to reduce vibration and noise in structures. Constrained layer damping (CLD) treatment has been proven to be an effective approach in suppressing excessive structural vibration to prevent structural damages or failures from operating in a dynamic environment. The damping treatment on the guiding vane of the inlet in the TF-30-P100 jet engine was one of the successful examples [1, 2]. The pioneering works about CLD on beams can be traced to DiTaranto [3] and Mead and Markus [4] for the axial and the bending vibration of beams. Since then, many papers were reported in this area for different structural elements, e.g., beams [5, 6], plates [7–9], shells [10–14], and rings [15]. Lately, Hu and Huang [16] developed a general theory for the constrained layer damping treatment, which can be applied to any other commonly encountered geometry.

[†]Ta Hwa Institute of Technology, 307, 1, Tahwa Road, ChiungLin, Hsinchu, Taiwan.
[‡]Nan Kai College, 568 Chung-Cheng Road, Tsao Tun, Nan Tou County, Taiwan.

0022-460X/02/$35.00

The responses of a circular plate subjected to traveling forces have been studied for years because of its importance to applications, e.g., circular saw, turbine rotor, and computer hard disk. However, the application of constrained layer damping treatment to circular plate was rather limited. Mirza and Singh [17] investigated the axisymmetric vibration of a circular sandwich plate in which the thick core layer was a low density and low strength material such as aluminum honeycomb. Roy and Ganesan [18] developed a finite element model for vibration and damping analysis of circular plates with constrained damping layer treatment. Both of the mentioned papers focused on the cases where the VEM layer was thicker than face layers.

The system considered herein consists of a three-layer annular plate with a viscoelastic core subjected to a spring–mass–dashpot (SMD) system rotating at constant angular velocity. Similar researches are as follows: Iwan and Stahl [19] analyzed a rigid disk of two/three degrees of freedom with a moving mass load. Hutton *et al.* [20] investigated the vibrations of a spinning saw blade with elastic supports. Shen and Mote Jr. [21] let the SMD circumnavigate the plate and discussed the influence of SMD parameters on system stability. Shen [22] demonstrated that axisymmetric plate damping will suppress the instability of plate/slider systems and the plate is modelled as Kelvin viscoelasticity of the circular plate. An important feature of the aforementioned work was the assumption that the SMD is treated as external loads. Huang and Hsu [23] employed the receptance method to solve for the modes of a spinning disk with point supports and obtained similar results with them.

The theoretical analysis begins with the derivation of governing equations for the three-layered annular plate. These equations are furthered reduced to three by eliminating the constraining layer displacements. The assumed-mode method is then employed to discretize the three equations. Next the receptance method is applied to combine the CLD plate and the rotating SMD system. The purpose of this study is to investigate the effect of the viscoelastic material (VEM) core and the dashpot on damping and frequencies of the CLD plate. In addition, the influence of the inertia and stiffness of the SMD on the dynamic response of the combined system are also examined.

2. EQUATIONS OF MOTION

Consider a physical system (Figure 1), consisting of a three-layer, annular plate with a viscoelastic core subjected to a linear SMD rotating at a constant speed Ω along a circle $r = r_0$. The host plate and the constraining layer (CL) are assumed to be homogenous,

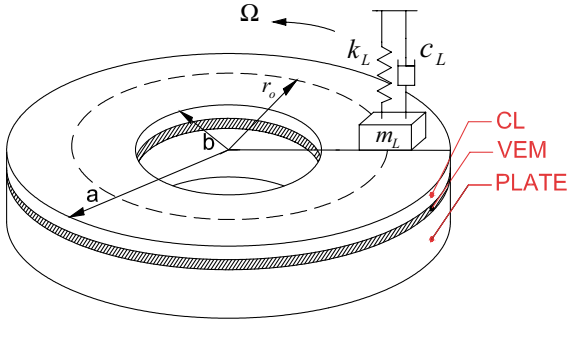

Figure 1. A schematic diagram of a CLD plate subject to an SMD system.

isotropic and elastic. The core made of VEM is the major damping mechanism for vibration suppression of the structure. The SMD- and CLD-treated plate are assumed to be in contact all the times. In the following, the plate and the SMD are treated as subsystems and the receptance method [24] is applied to join the subsystems.

First, the governing equations of a CLD-treated plate clamped inside and free outside subjected to a harmonic load traveling in circumferential direction are derived. The symbols h, ρ, E, and μ denote thickness, density, Young's modulus, and the Poisson ratio respectively. The superscripts p, c, and v are designated for the plate, the CL, and the VEM respectively. Based on the thin shell theory, Love's assumptions, and the no-slip constrains (displacement continuity) between layers, i.e.,

$$\begin{aligned} u_j^v(r,\theta) &= \frac{1}{2}\left[\left(u_j^c - \frac{h^c}{2}\beta_j^c\right) + \left(u_j^p + \frac{h^p}{2}\beta_j^p\right)\right], \\ \beta_j^v(r,\theta) &= \frac{1}{h^v}\left[\left(u_j^c - \frac{h^c}{2}\beta_j^c\right) - \left(u_j^p + \frac{h^p}{2}\beta_j^p\right)\right], \end{aligned} \quad j = r,\theta, \tag{1}$$

the equations of motion and the boundary conditions, are derived via Hamilton's principle. Note that β_j^c and β_j^p in equation (1) are the rotation angles, expressed in Appendix A. The Donnell–Mushtari–Vlasov assumptions [24] further simplify the equations to be

$$\begin{aligned} &-\frac{\partial}{\partial r}(N_{rr}^c r) + N_{\theta\theta}^c - \frac{\partial}{\partial\theta}(N_{r\theta}^c) - \frac{\partial}{\partial r}\left[\left(\frac{N_{rr}^v}{2} + \frac{M_{rr}^v}{h^v}\right)r\right] + \left(\frac{N_{\theta\theta}^v}{2} + \frac{M_{\theta\theta}^v}{h^v}\right) + \frac{Q_{rz}^v r}{h^v} = 0, \\ &-\frac{\partial}{\partial\theta}(N_{\theta\theta}^c) - \frac{\partial}{\partial r}(N_{r\theta}^c r) - N_{r\theta}^c - \frac{\partial}{\partial\theta}\left(\frac{N_{\theta\theta}^v}{2} + \frac{M_{\theta\theta}^v}{h^v}\right) + \frac{Q_{\theta z}^v r}{h^v} = 0, \\ &-\frac{\partial}{\partial r}(N_{rr}^p r) + N_{\theta\theta}^p - \frac{\partial}{\partial\theta}(N_{r\theta}^p) - \frac{\partial}{\partial r}\left[\left(\frac{N_{rr}^v}{2} - \frac{M_{rr}^v}{h^v}\right)r\right] + \left(\frac{N_{\theta\theta}^v}{2} - \frac{M_{\theta\theta}^v}{h^v}\right) - \frac{Q_{rz}^v r}{h^v} = 0, \\ &-\frac{\partial}{\partial\theta}(N_{\theta\theta}^p) - \frac{\partial}{\partial r}(N_{r\theta}^p r) - N_{r\theta}^p - \frac{\partial}{\partial\theta}\left(\frac{N_{\theta\theta}^v}{2} - \frac{M_{\theta\theta}^v}{h^v}\right) - \frac{Q_{\theta z}^v r}{h^v} = 0, \\ &-\frac{\partial}{\partial r}(Q_{rz}^c r) - \frac{\partial}{\partial\theta}(Q_{\theta z}^c) - \frac{\partial}{\partial r}(Q_{rz}^p r) - \frac{\partial}{\partial\theta}(Q_{\theta z}^p) - \frac{\partial}{\partial r}(Q_{rz}^v r) - \frac{\partial}{\partial\theta}(Q_{\theta z}^v) \\ &\quad + \rho^c h^c r\ddot{u}_z + \rho^p h^p r\ddot{u}_z + \rho^v h^v r\ddot{u}_z = r q_z^c, \end{aligned} \tag{2}$$

where Q_{rz}^c, $Q_{\theta z}^c$, Q_{rz}^p, and $Q_{\theta z}^p$, the shear resultants, satisfy the following equations:

$$\begin{aligned} &-\frac{\partial}{\partial r}(M_{rr}^c r) + M_{\theta\theta}^c - \frac{\partial}{\partial\theta}(M_{r\theta}^c) + Q_{rz}^c r + \frac{\partial}{\partial r}\left[\frac{h^c r}{2}\left(\frac{N_{rr}^v}{2} + \frac{M_{rr}^v}{h^v}\right)\right] \\ &\quad - \frac{h^c}{2}\left(\frac{N_{\theta\theta}^v}{2} + \frac{M_{\theta\theta}^v}{h^v}\right) - \frac{h^c}{2h^v}Q_{rz}^v r = 0, \\ &-\frac{\partial}{\partial\theta}(M_{\theta\theta}^c) - \frac{\partial}{\partial r}(M_{r\theta}^c r) - M_{r\theta}^c + Q_{\theta z}^c r + \frac{\partial}{\partial\theta}\left[\frac{h^c}{2}\left(\frac{N_{\theta\theta}^v}{2} + \frac{M_{\theta\theta}^v}{h^v}\right)\right] - \frac{h^c}{2h^v}Q_{\theta z}^v r = 0, \\ &-\frac{\partial}{\partial r}(M_{rr}^p r) + M_{\theta\theta}^p - \frac{\partial}{\partial\theta}(M_{r\theta}^p) + Q_{rz}^p r - \frac{\partial}{\partial r}\left[\frac{h^p r}{2}\left(\frac{N_{rr}^v}{2} - \frac{M_{rr}^v}{h^v}\right)\right] \\ &\quad + \frac{h^p}{2}\left(\frac{N_{\theta\theta}^v}{2} - \frac{M_{\theta\theta}^v}{h^v}\right) - \frac{h^p}{2h^v}Q_{rz}^v r = 0, \\ &-\frac{\partial}{\partial\theta}(M_{\theta\theta}^p) - \frac{\partial}{\partial r}(M_{r\theta}^p r) - M_{r\theta}^p + Q_{\theta z}^p r - \frac{\partial}{\partial\theta}\left[\frac{h^p}{2}\left(\frac{N_{\theta\theta}^v}{2} - \frac{M_{\theta\theta}^v}{h^v}\right)\right] - \frac{h^p}{2h^v}Q_{\theta z}^v r = 0. \end{aligned} \tag{3}$$

The expressions of membrane forces N's, bending moments M's, and shear force resultants Q's are given in Appendix A, equations (A2–A6). The boundary conditions for

an $r=$constant edge are derived to be

$$
\begin{aligned}
&u_r^c = u_r^{c*} \quad \text{or} \quad N_{rr}^c + \left(\frac{N_{rr}^v}{2} + \frac{M_{rr}^v}{h^v}\right) = N_{rr}^{c*} + \left(\frac{N_{rr}^{v*}}{2} + \frac{M_{rr}^{v*}}{h^v}\right),\\
&u_\theta^c = u_\theta^{c*} \quad \text{or} \quad N_{r\theta}^c = N_{\theta r}^{c*},\\
&u_r^p = u_r^{p*} \quad \text{or} \; N_{rr}^p + \left(\frac{N_{rr}^v}{2} - \frac{M_{rr}^v}{h^v}\right) = N_{rr}^{p*} + \left(\frac{N_{rr}^{v*}}{2} - \frac{M_{rr}^{v*}}{h^v}\right),\\
&u_\theta^p = u_\theta^{p*} \quad \text{or} \quad N_{r\theta}^p = N_{\theta r}^{p*},\\
&u_z = u_z^* \quad \text{or} \quad Q_{rz}^c + Q_{rz}^p + Q_{rz}^v + \frac{\partial M_{r\theta}^c}{r\partial\theta} + \frac{\partial M_{r\theta}^p}{r\partial\theta}\\
&\qquad\qquad = Q_{rz}^{c*} + Q_{rz}^{p*} + Q_{rz}^{v*} + \frac{\partial M_{r\theta}^{c*}}{r\partial\theta} + \frac{\partial M_{r\theta}^{p*}}{r\partial\theta},\\
&\frac{\partial u_z}{\partial r} = \left(\frac{\partial u_z}{\partial r}\right)^* \quad \text{or} \quad M_{rr}^c + M_{rr}^p - \frac{h^c}{2}\left(\frac{N_{rr}^v}{2} + \frac{M_{rr}^v}{h^v}\right) + \frac{h^p}{2}\left(\frac{N_{rr}^v}{2} - \frac{M_{rr}^v}{h^v}\right)\\
&\qquad\qquad = M_{rr}^{c*} + M_{rr}^{p*} - \frac{h^c}{2}\left(\frac{N_{rr}^{v*}}{2} + \frac{M_{rr}^{v*}}{h^v}\right) + \frac{h^p}{2}\left(\frac{N_{rr}^{v*}}{2} - \frac{M_{rr}^{v*}}{h^v}\right).
\end{aligned}
\tag{4}
$$

Similarly, the boundary conditions for a $\theta=$constant are

$$
\begin{aligned}
&u_r^c = u_r^{c*} \quad \text{or} \quad N_{r\theta}^c = N_{\theta r}^{c*},\\
&u_\theta^c = u_r^{c*} \quad \text{or} \quad N_{\theta\theta}^c + \left(\frac{N_{\theta\theta}^v}{2} + \frac{M_{\theta\theta}^v}{h^v}\right) = N_{\theta\theta}^{c*} + \left(\frac{N_{\theta\theta}^{v*}}{2} + \frac{M_{\theta\theta}^{v*}}{h^v}\right),\\
&u_r^p = u_r^{p*} \quad \text{or} \quad N_{r\theta}^p = N_{\theta r}^{p*},\\
&u_\theta^p = u_r^{p*} \quad \text{or} \quad N_{\theta\theta}^p + \left(\frac{N_{\theta\theta}^v}{2} - \frac{M_{\theta\theta}^v}{h^v}\right) = N_{\theta\theta}^{p*} + \left(\frac{N_{\theta\theta}^{v*}}{2} - \frac{M_{\theta\theta}^{v*}}{h^v}\right),\\
&u_z = u_z^* \quad \text{or} \quad Q_{\theta z}^c + Q_{\theta z}^p + Q_{\theta z}^v + \frac{\partial M_{r\theta}^c}{\partial r} + \frac{\partial M_{r\theta}^p}{\partial r}\\
&\qquad\qquad = Q_{\theta z}^{c*} + Q_{\theta z}^{p*} + Q_{\theta z}^{v*} + \frac{\partial M_{r\theta}^{c*}}{\partial r} + \frac{\partial M_{r\theta}^{p*}}{\partial r},\\
&\frac{1}{r}\frac{\partial u_z}{\partial\theta} = \frac{1}{r}\left(\frac{\partial u_z}{\partial\theta}\right)^* \quad \text{or} \quad M_{\theta\theta}^c + M_{\theta\theta}^p - \frac{h^c}{2}\left(\frac{N_{\theta\theta}^v}{2} + \frac{M_{\theta\theta}^v}{h^v}\right) + \frac{h^p}{2}\left(\frac{N_{\theta\theta}^v}{2} - \frac{M_{\theta\theta}^v}{h^v}\right)\\
&\qquad\qquad = M_\theta^{c*} + M_\theta^{p*} - \frac{h^c}{2}\left(\frac{N_{\theta\theta}^{v*}}{2} + \frac{M_{\theta\theta}^{v*}}{h^v}\right) + \frac{h^p}{2}\left(\frac{N_{\theta\theta}^{v*}}{2} - \frac{M_{\theta\theta}^{v*}}{h^v}\right).
\end{aligned}
\tag{5}
$$

Neglecting the in-plane normal strains of the VEM layer, this results in the constraining layer displacements, u_r^c and u_θ^c, in the above equations being eliminated. Subsequently, the number of equations reduces to three, and are in terms of plate displacements,

u_r^p, u_θ^p and u_z only,

$$\frac{k^p h^v}{G^v}\left\{-\frac{3\partial^2 u_r^p}{r\partial r^2}+\frac{3\partial u_r^p}{r^2\partial r}+\frac{2\partial^3 u_r^p}{\partial r^3}-\frac{3u_r^p}{r^3}+\frac{r\partial^4 u_r^p}{\partial r^4}+c_a\frac{\partial^3 u_r^p}{r^2\partial r\partial\theta^2}+c_b\frac{\partial^2 u_r^p}{r^3\partial\theta^2}\right.$$
$$+c_c\frac{\partial^2 u_\theta^p}{r^2\partial r\partial\theta}+c_d\frac{\partial u_\theta^p}{r^3\partial\theta}+c_e\frac{\partial^3 u_\theta^p}{r\partial r^2\partial\theta}+c_f\frac{\partial^4 u_r^p}{r\partial r^2\partial\theta^2}+c_g\frac{\partial^4 u_\theta^p}{\partial r^3\partial\theta}+c_h\frac{\partial^4 u_r^p}{r^3\partial\theta^4}$$
$$\left.+c_i\frac{\partial^3 u_\theta^p}{r^3\partial\theta^3}+c_j\frac{\partial^4 u_\theta^p}{r^2\partial r\partial\theta^3}\right\}-c_k\left(\frac{u_r^p}{r}-\frac{\partial u_r^p}{\partial r}-\frac{r\partial^2 u_r^p}{\partial r^2}\right)-c_l\frac{\partial^2 u_r^p}{r\partial\theta^2}+c_m\frac{\partial u_\theta^p}{r\partial\theta}$$
$$-c_n\frac{\partial^2 u_\theta^p}{\partial r\partial\theta}+\frac{h^c+h^p+2h^v}{2}\left\{\frac{\partial^2 u_z}{\partial r^2}+\frac{r\partial^3 u_z}{\partial r^3}-\frac{\partial u_z}{r\partial r}+\frac{\partial^3 u_z}{r\partial r\partial\theta^2}-\frac{2\partial^2 u_z}{r^2\partial\theta^2}\right\}=0, \tag{6}$$

$$\frac{k^p h^v}{G^v}\left\{-\frac{\partial^4 u_\theta^p}{r^3\partial\theta^4}+d_a\frac{\partial^3 u_r^p}{r\partial r^2\partial\theta}+d_b\left(\frac{\partial^2 u_r^p}{r^2\partial r\partial\theta}-\frac{\partial u_r^p}{r^3\partial\theta}\right)+d_c\frac{\partial^4 u_r^p}{\partial r^3\partial\theta}+d_d\frac{\partial^4 u_r^p}{r^2\partial r\partial\theta^3}\right.$$
$$+d_e\frac{\partial^3 u_r^p}{r^3\partial\theta^3}+d_f\frac{\partial^3 u_\theta^p}{r^2\partial r\partial\theta^2}+d_g\frac{\partial^2 u_\theta^p}{r^3\partial\theta^2}+d_h\frac{\partial^4 u_\theta^p}{r\partial r^2\partial\theta^2}-d_i\left(\frac{2\partial^3 u_\theta^p}{\partial r^3}+\frac{r\partial^4 u_\theta^p}{\partial r^4}\right)$$
$$\left.+d_j\left(\frac{\partial^2 u_\theta^p}{r\partial r^2}-\frac{\partial u_\theta^p}{r^2\partial r}+\frac{u_\theta^p}{r^3}\right)\right\}+d_k\frac{\partial^2 u_r^p}{\partial r\partial\theta}+d_l\frac{\partial u_r^p}{r\partial\theta}+d_m\frac{\partial^2 u_\theta^p}{r\partial\theta^2}$$
$$+d_n\left(\frac{r\partial^2 u_\theta^p}{\partial r^2}-\frac{u_\theta^p}{r}+\frac{\partial u_\theta^p}{\partial r}\right)-\frac{h^c+h^p+2h^v}{2}\left\{\frac{\partial^3 u_z}{\partial r^2\partial\theta}+\frac{\partial^2 u_z}{r\partial r\partial\theta}+\frac{\partial^3 u_z}{r^2\partial\theta^3}\right\}=0, \tag{7}$$

$$\frac{(h^c+h^p+2h^v)k^p}{2}\left\{\frac{\partial u_r^p}{r^2\partial r}-\frac{2\partial^2 u_r^p}{r\partial r^2}-\frac{u_r^p}{r^3}-\frac{\partial^3 u_r^p}{\partial r^3}-\frac{\partial^3 u_\theta^p}{r^3\partial\theta^3}-\frac{\partial^2 u_r^p}{r^3\partial\theta^2}-\frac{\partial u_\theta^p}{r^3\partial\theta}+\frac{\partial^2 u_\theta^p}{r^2\partial r\partial\theta}\right.$$
$$\left.-\frac{\partial^3 u_r^p}{r^2\partial r\partial\theta^2}-\frac{\partial^3 u_\theta^p}{r\partial r^2\partial\theta}\right\}-(D^c+D^p)\nabla^4 u_z-(\rho^c h^c+\rho^p h^p+\rho^v h^v)\ddot{u}_z=q_z^c, \tag{8}$$

where the coefficients $c_a, c_b, \ldots, c_n$ and $d_a, d_b, \ldots, d_n$ are shown in Appendix A, (A7–A8).

A unit harmonic, traveling point load can be expressed as

$$q_z^c(r,\theta,t)=\frac{1}{r}\delta(r-r_0)\delta(\theta-\Omega t)e^{i\omega t}, \tag{9}$$

where $(r_0, \Omega t)$ locates the loading position and ω is the excitation frequency. The response of a rotating disk due to a traveling point load such as equation (9) is of practical interest. For example, modelling a memory disk drive in a computer system or a rotating slider bearing system enables the full comprehension of its dynamic behaviors and provides some design consideration.

Due to the complexity of the equations, the assumed modes method is hence applied. The displacement functions are assumed to be

$$u_r^p(r,\theta,t)=\sum_{m=0}^{M}\sum_{n=0}^{N}[\alpha_{mn}(t)\cos(n\theta)+\psi_{mn}(t)\sin(n\theta)]\sin\left(\frac{(m+1)(r-b)\pi}{2l}\right),$$
$$u_\theta^p(r,\theta,t)=\sum_{m=0}^{M}\sum_{n=0}^{N}[\varphi_{mn}(t)\sin(n\theta)+\phi_{mn}(t)\cos(n\theta)]\sin\left(\frac{(m+1)(r-b)\pi}{2l}\right),$$
$$u_z(r,\theta,t)=\sum_{m=0}^{M}\sum_{n=0}^{N}[\zeta_{mn}(t)\cos(n\theta)+\beta_{mn}(t)\sin(n\theta)]R_{mn}(r), \tag{10a - c}$$

where $\alpha_{mn}(t)$, $\psi_{mn}(t)$, $\varphi_{mn}(t)$, $\phi_{mn}(t)$, $\zeta_{mn}(t)$, and $\beta_{mn}(t)$ are the generalized co-ordinates, n and m are the circumferential and the radial wave numbers, respectively; $l=a-b$; $R_{mn}(r)$

is chosen as the polynomial functions in the present cases, i.e.,

$$R_{mn}(r) = P_{mn}(r-b)^{m+2} + Q_{mn}(r-b)^{m+3} + R_{mn}(r-b)^{m+4}, \tag{11}$$

P_{mn}, Q_{mn}, and R_{mn} are coefficients chosen such that equation (11) satisfies the boundary equations. Note that in equations (10) and (11), m (nodal circle number) is assumed to range from zero to infinite. Yet, for most of the vibration cases the modes associated with an m number larger than 0, i.e., $m \geqslant 1$, are just slightly excited compared to $m = 0$ modes [20]. To save computation time, only the $m = 0$ terms are considered in the following analyses.

Substituting equation (10) into equations (6)–(8) and utilizing the orthogonality of trigonometric functions, a set of discretized equations for each n number is obtained:

$$\begin{aligned} \mathbf{M}_n\ddot{\mathbf{X}}_{an} + \mathbf{K}_n\mathbf{X}_{an} &= \mathbf{Q}_{an}, \\ \mathbf{M}_n\ddot{\mathbf{X}}_{bn} + \mathbf{K}_n\mathbf{X}_{bn} &= \mathbf{Q}_{bn}, \end{aligned} \quad n = 0, 1, 2, \ldots, N, \tag{12a, b}$$

where $\mathbf{M}_n$, $\mathbf{K}_n$, $\mathbf{X}_{an}$, $\mathbf{X}_{bn}$, $\mathbf{Q}_{an}$, and $\mathbf{Q}_{bn}$ are

$$\mathbf{M}_n = \begin{bmatrix} 0 & 0 & 0 \\ 0 & 0 & 0 \\ 0 & 0 & m_n \end{bmatrix}, \quad \mathbf{K}_n = \begin{bmatrix} k_{11}(n) & k_{12}(n) & k_{13}(n) \\ k_{21}(n) & k_{22}(n) & k_{23}(n) \\ k_{31}(n) & k_{32}(n) & k_{33}(n) \end{bmatrix}, \tag{13}$$

$$\mathbf{X}_{an} = \{\alpha_n(t), \varphi_n(t), \zeta_n(t)\}^{\mathrm{T}}, \quad \mathbf{X}_{bn} = \{\psi_n(t), \phi_n(t), \beta_n(t)\}^{\mathrm{T}}, \tag{14}$$

$$\mathbf{Q}_{an} = \{0, 0, q_1(t)\}^{\mathrm{T}}, \quad \mathbf{Q}_{bn} = \{0, 0, q_2(t)\}^{\mathrm{T}}. \tag{15}$$

Note that the expressions of m_n,$k_{ij}(n)$, and q_i are given in detail in Appendix A, equations (A9–A12).

Since the in-plane inertia have been neglected, the first two equations in the matrix equations (12a,b) are in fact the static equilibrium equations. Therefore, equations (12a,b) can be rearranged such that the dynamic behavior is merely in terms of the transverse displacement as shown below,

$$\begin{aligned} m_n\ddot{\zeta}_n + k_n\zeta_n &= q_1, \\ m_n\ddot{\beta}_n + k_n\beta_n &= q_2, \end{aligned} \quad n = 0, 1, 2, \ldots, N, \tag{16}$$

where

$$k_n = k_{33} + \frac{k_{31}(k_{12}k_{23} + k_{13}k_{22}) - k_{32}(k_{13}k_{21} + k_{11}k_{23})}{k_{11}k_{22} - k_{12}k_{21}}. \tag{17}$$

To study the harmonic steady state response, the properties of VEM, in a usual manner, are assumed to be

$$G^v = G_0^v(1 + \mathrm{i}\eta), \tag{18}$$

where G_0^v is the storage modulus and η is the loss factor. The plate's response yields via superimposing each n's modal response. The eigenvalue of equation (16) can be expressed as

$$\lambda = d + \mathrm{i}e. \tag{19}$$

The real part of λ is the system's resonant frequency. The ratio of the imaginary to the real is the damping ratio, i.e.,

$$\xi = \frac{e/d}{\sqrt{1 + (e/d)^2}}. \tag{20}$$

For the case of a stationary (non-rotating) harmonic point load, the response is solved to be

$$u_z(r,\theta,t)=\sum_{n=0}^{N}\frac{\chi_n}{k_n-m_n\omega^2}\frac{1}{\pi}\cos n(\theta-\theta_0)R_n(r)R_n(r_0)\mathrm{e}^{\mathrm{i}\omega t},\ \chi_n=\begin{cases}1/2, & n=0,\\ 1, & n\neq 0.\end{cases}\tag{21}$$

Secondly, the steady state response due to a rotating, harmonic point load is obtained as well,

$$u_z(r,\theta,t)=\sum_{n=0}^{N}\left\{\frac{\chi_n\mathrm{e}^{\mathrm{i}[\omega_1 t-n\theta]}}{k_n-m_n\omega_1^2}+\frac{\chi_n\mathrm{e}^{\mathrm{i}[\omega_2 t+n\theta]}}{k_n-m_n\omega_2^2}\right\}\frac{R_n(r_0)R_n(r)}{2\pi},\quad \chi_n=\begin{cases}1/2, & n=0,\\ 1, & n\neq 0.\end{cases}\tag{22}$$

Note that the driving frequencies to the plate, $\omega_{1,2}=\omega\pm n\Omega$, are the combinations of the harmonic frequency and the rotational speed. This is a peculiar feature of a traveling load.

3. VIBRATIONS OF A PLATE WITH AN SMD SYSTEM

The receptance method is to be applied to join the plate and the SMD system. A detailed description about receptance method can be found in reference [24]. The connection between the plate and the SMD is treated as one-junction and the frequency equation of the joined systems is

$$\alpha_{11}+\beta_{11}=0,\tag{23}$$

where α_{11} denotes the direct receptance of the SMD and β_{11} is that of the plate. The complex receptance of the SMD system is

$$\alpha_{11}=\frac{1}{k_L+\mathrm{i}c_L\omega-m_L\omega^2},\tag{24}$$

where m_L, c_L, and k_L are the inertia, damping, and stiffness coefficients. The direct receptance of the plate for two different cases are obtained, respectively, as

$$\beta_{11}=\sum_{n=0}^{N}\frac{\chi_n}{k_n-m_n\omega^2}\frac{R_n^2(r_0)}{\pi}\quad\text{for a stationary, harmonic point load}\tag{25}$$

and

$$\beta_{11}=\sum_{n=0}^{N}\left[\frac{1}{k_n-m_n\omega_1^2}+\frac{1}{k_n-m_n\omega_2^2}\right]\frac{\chi_n R_n^2(r_0)}{2\pi}\quad\text{for a traveling, harmonic load.}\tag{26}$$

Then the frequency equation for the plate contacting to a stationary SMD system is

$$\sum_{n=0}^{N}\frac{\chi_n}{k_n-m_n\omega^2}\frac{R_n^2(r_0)}{\pi}+\frac{1}{k_L+\mathrm{i}c_L\omega-m_L\omega^2}=0\tag{27}$$

and for the case of a traveling SMD system, the equation is

$$\sum_{n=0}^{N}\left[\frac{1}{k_n-m_n\omega_1^2}+\frac{1}{k_n-m_n\omega_2^2}\right]\frac{\chi_n R_n^2(r_0)}{2\pi}+\frac{1}{k_L+\mathrm{i}c_L\omega-m_L\omega^2}=0.\tag{28}$$

In the following, the geometry and material properties for the numerical examples are given in Table 1. The VEM property is adopted directly from Kerwin's model

TABLE 1

Geometry and material properties of the CLD circular plate

Thickness	$h^p = 1$ mm
Radia	inner radius $b = 18$ mm, outer radius $a = 60$ mm
Face layers (aluminum)	$E^p = E^c = 70$ Gpa, $\mu^p = \mu^c = 0{\cdot}3$, $\rho^p = \rho^c = 2710$ Kg/m^3
VEM (polymer)	$\rho^v = 1340$ Kg/m^3, $G^v = (6, 3)$ Mpa

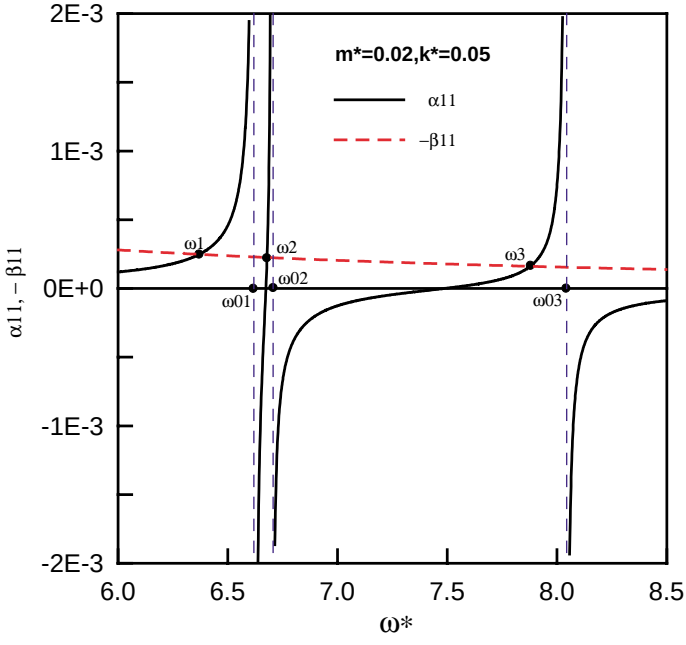

Figure 2. Graphical method for finding the natural frequencies of the bare plate with SM system.

[18]. Dimensionless inertia m^* and stiffness k^* are defined as follows:

$$m^* = \frac{m_L}{M}, \quad k^* = k_L \frac{a^2}{D^p}, \tag{29}$$

where M is the mass of the CLD plate.

The objective of this research is to realize which is the very effective way of imposing damping on system. The characteristics of the bare plate contacted to an SM system are used as a base for comparison. The effect of damping once added in the plate via VEM and once added in SM to form SMD is then discussed. In the following, the parameters m^* and k^* are set to be 0·02 and 0·05 and a dimensionless frequency ω^* is normalized in such a way that

$$\omega^* = \omega \sqrt{\frac{\rho^p h^p a^4}{D^p}}. \tag{30}$$

The frequencies, said ω_p's, that satisfy equation (27) are the natural frequencies of the combined system. They can be solved either numerically or graphically. In a graphical

method, one seeks for the intersections of the curves α_{11} and $-\beta_{11}$ as illustrated in Figure 2. From Figure 2 it is seen that the combined system's natural frequencies ω_i's are smaller than those ω_{0i}'s of the plate.

Next, the frequency and damping variations are studied numerically. Since the treatment thickness of the treated plate is usually limited in engineering applications, the total thickness of CLD treatment is set to be 20% of the host plate's in the following examples. The damping ratio of the dashpot is chosen as 0·1. Figure 3(a) displays the frequency curves, in which the dash curve represents the bare plate. It is solved via assuming h^v and h^c are equal to zero in the CLD plate model. The data is very consistent with that from the conventional plate theory [25], and it can be a partial check of the developed theory. As seen from the figure, the other two curves, one with SMD and one

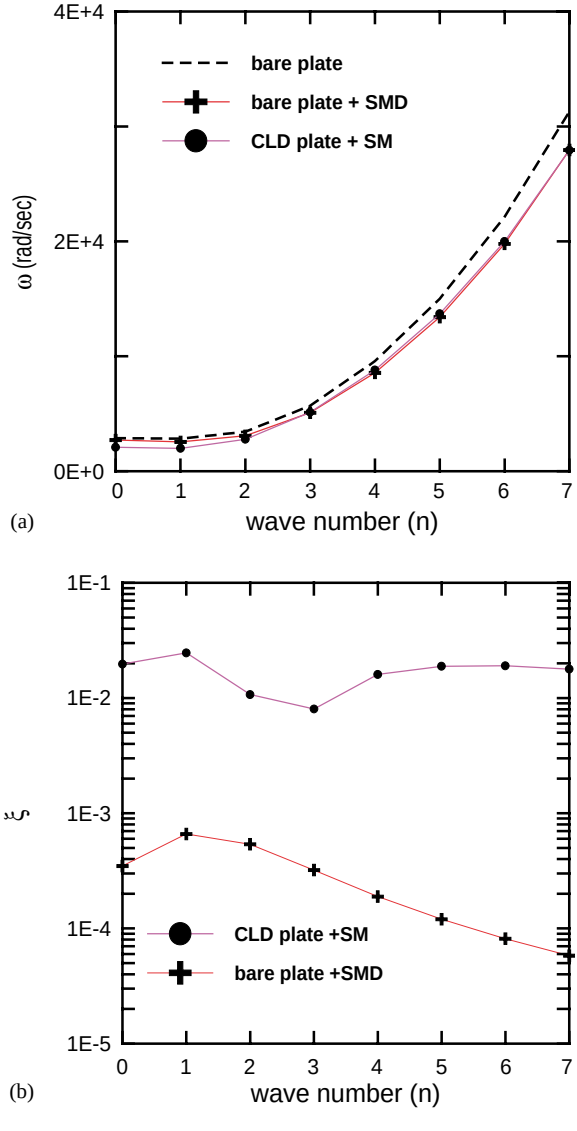

Figure 3. (a) Variations of frequencies for different plate systems. (b) Variations of damping ratios for different plate systems.

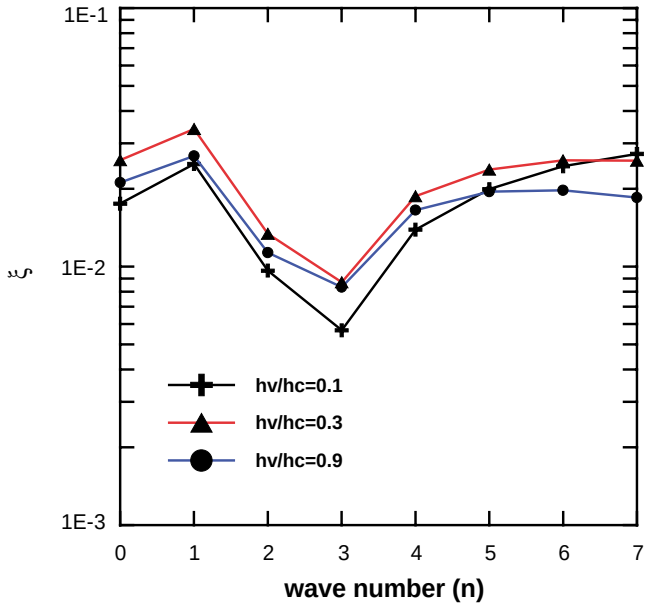

Figure 4. Variations of damping ratios for different thickness ratios.

with CLD, deviate from the bare plate just slightly. The difference becomes obvious at higher modes. The damping ratios for two systems are compared in Figure 3(b). It is seen that damping due to the VEM layer is larger than that due to SMD. This difference is attributed to the VEM layer being fully covered over the plate. Although the SMD provides large damping through the dashpot, it acts just on a single point. It shows that the $n = 1$ mode has the maximum damping in both cases. Since the damping caused by CLD is significantly larger than the dashpot, we will focus on the CLD damping treatment hereafter.

Figure 4 shows the damping ratios of individual modes with three different thickness ratios h^v/h^c under the constraint of $h^v + h^c = 0{\cdot}2$ mm. It is to look into the influence of damping effect subject to the variation of thickness ratio h^v/h^c. As seen from the figure, the increase of VEM layer thickness does not necessarily improve the damping effect. This result is conceptually realized since the total treatment thickness is restricted and increases of VEM results in decrease of CL that consequently reduces CL's rigidity. The results are consistent with the other investigation [15]. The present results show that $h^v/h^c = 0{\cdot}3$ possesses the largest damping effect among the shown cases.

At last, the responses due to traveling harmonic SM of a driving frequency ω and a rotational speed Ω applying at the plate is demonstrated. This simulates a disk–head system. Figure 5 shows the resonant frequency curves as functions of ω and Ω for $n = 1-3$ modes. These figures attempt to show how the frequency ω and the rotational speed Ω are affected by the stiffness k^* and the inertia m^*. It is discovered that the attachment of k^* affects the plate's frequencies slightly, but it bifurcates the original frequency at $\Omega = 0$ into two. The lower frequency remains that of the plate. The bifurcation is attributed to that there are two modes, said $\cos n\theta$ and $\sin n\theta$ associated with every frequency, i.e., repeated frequency, for a symmetric plate. The attachment of SM destroys the symmetry such that the plate orients itself so that the attaching point becomes a node for one case and an antinode for the other case (the higher frequency). As to m^*, the influence is very

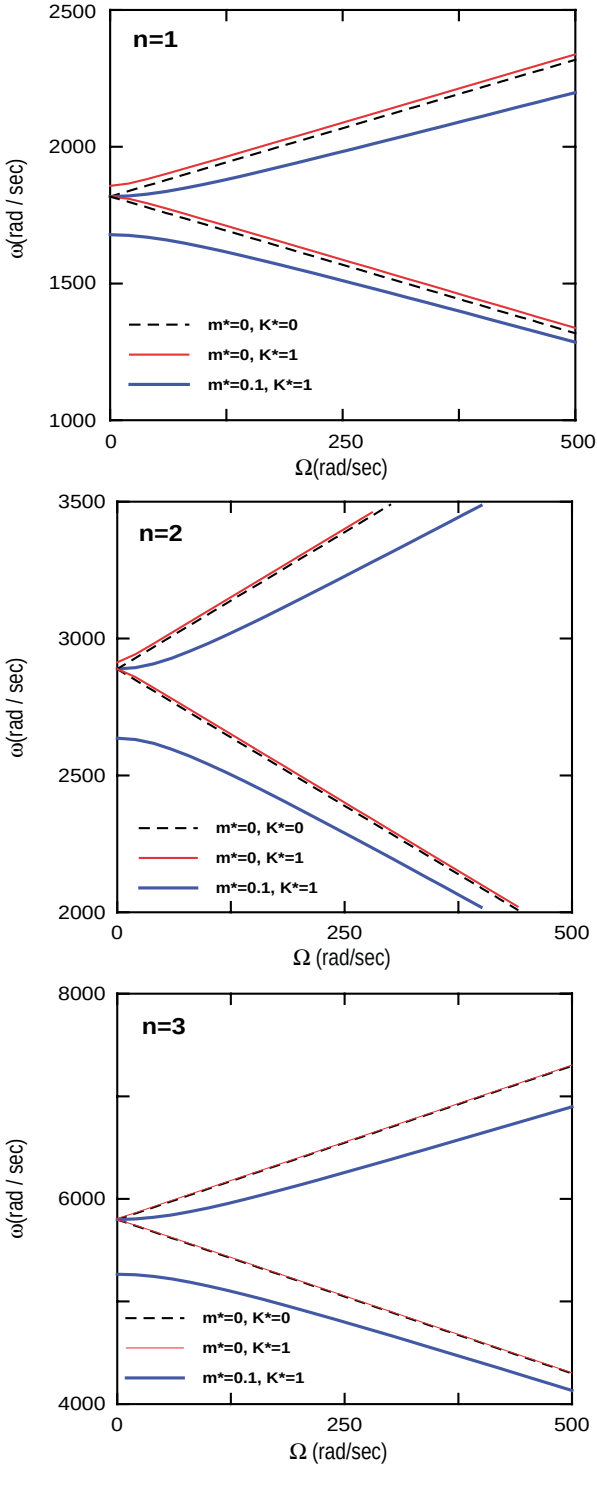

Figure 5. The resonant curves for the $n = 1-3$ modes.

significant. The figure also shows that the increase of Ω leads to the system's natural frequencies moving farther away of the plate's.

Figure 6 illustrates in more detail the variation of the frequency and the damping ratios to the rotational speed for the $n = 0-3$ modes. As revealed by Figure 6(a), the traveling SM system bifurcates each $n \neq 0$ resonant frequency into two, one is the so-called forward wave and the other is the backward wave. The (0,0) mode, also called the flapping mode, is not bifurcated by the rotational speed due to its non-repeated frequency. Figure 6(b) shows the damping ratios of forward and backward traveling waves. The figure indicates

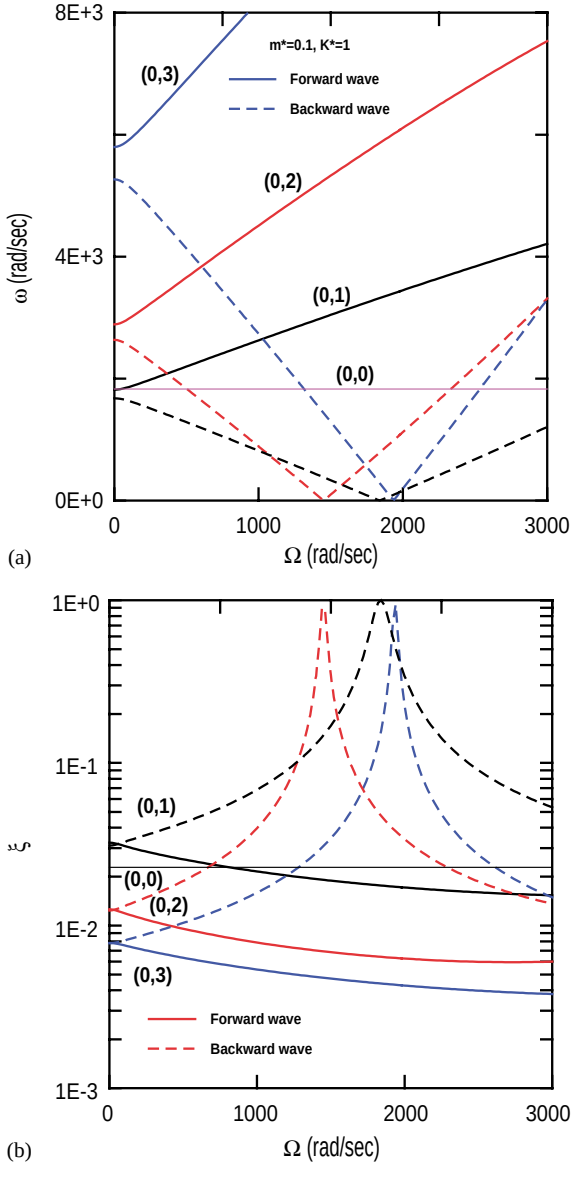

Figure 6. (a). Variations of frequencies of the combined system on the rotational speed. (b) Variations of damping ratios of the combined system on the rotational speed.

that the damping of the backward wave is higher than that of the forward wave. The damping of the forward wave decreases with the increase of rotational speed. The damping of the backward wave increases with the rotational speed at the beginning. It reaches a maximum at the critical point, where backward wave approaches zero, and then decreases with the rotational speed.

4. CONCLUSIONS

The vibration and damping characteristics of an annular plate with constrained layer damping treatment subject to a traveling SMD were investigated. The governing equations of the CLD-treated plate were first derived via Hamilton's principle. These equations were furthered reduced to three only in terms of the host plate's displacements. The receptance method followed to joint the stationary CLD plate and the rotating SMD. From the examples illustrated, the authors have arrived at the following conclusions. (1) The passive constrained layer damping treatment was a more effective approach than the dashpot in reducing the response amplitude. The results proved the damping ratios of the combined system due to viscous damper were lower than that from the viscoelastic core. (2) There exists a best design on the thickness ratio of the VEM core to constraining layer to have the maximum damping effects. (3) When the SM was attached to the plate, the plate's frequencies bifurcated except for the $n = 0$ mode. The attached inertia has very significant influence on the resonance frequency of the plate but not the stiffness. (4) The damping ratios of the backward waves were higher than those of the forward waves.

REFERENCES

1. L. C. Rogers and M. L. Parin 1978 *AFFDL-TM-78-FBA*, 227–293. A thoroughly engineering application of damping technology to jet engine inlet guide vanes.
2. J. P. Henderson, M. L. Parin, L. C. Rogers and D. B. Paul 1979 *American Society of Mechanical Engineers Paper No.* 79-*GT*-163. Engine evaluation of a vibration damping treatment for inlet guide vanes.
3. R. A. DiTaranto 1965 *Transaction of the American Society of Mechanical Engineers, Series E* **87**, 881–886. Theory of vibratory bending for elastic and viscoelastic layered finite-length beams.
4. D. J. Mead and S. Markus 1969 *American Institute of Aeronautics and Astronautics Journal* **10**, 163–175. The forced vibration of a three-layer, damped sandwich beam with arbitrary boundary conditions.
5. B. E. Douglas and J. C. S. Yang 1978 *American Institute of Aeronautics and Astronautics Journal* **16**, 925–930. Transverse compressional damping in the vibratory response of elastic–viscoelastic beams.
6. S. C. Huang, D. J. Inman, and E. M. Austin 1995 *Journal of Smart Material and Structure* **5**, 301–313. Some design considerations for active and passive constrained layer damping treatments.
7. M. J. Yan and E. H. Dowell 1972 *American Society of Mechanical Engineers Journal of Applied Mechanics* **39**, 1041–1046. Governing equations of vibrating constrained-layer damping sandwich plates and beams.
8. D. J. Mead and Y. Yaman 1991 *Journal of Sound and Vibration* **145**, 409–428. The harmonic response of rectangular sandwich plates with multiple stiffening: a flexural wave analysis.
9. Y. C. Chen and S. C. Huang 1998 *Journal of Wave–Material Interaction* **13**, 34–57. A simplified theory for the vibration of plates with CLD treatment.
10. M. Ei-Raheb and P. Wagner 1986 *American Society of Mechanical Engineers Journal of Applied Mechanics* **53**, 902–908. Damped response of shells by a constrained viscoelastic layer.

11. Y. P. Lu, A. J. Roscoe, and B. E. Douglas 1991 *Journal of Sound and Vibration* **150**, 395–403. Analysis of the response of damped cylindrical shells carrying discontinuously constrained beam elements.
12. T. C. Ramesh and N. Ganesan 1994 *Journal of Sound and Vibration* **175**, 535–555. Orthotropic cylindrical shells with a viscoelastic core: a vibration and damping analysis.
13. L. H. Chen and S. C. Huang 1999 *International Journal of Mechanical Sciences* **41**, 1485–1498. Vibration of a cylindrical shell with partially constrained layer damping (CLD) treatment.
14. Y. C. Hu and S. C. Huang 2000 *Computers & Structures* **76**, 577–591. The frequency response and damping effect of three-layer thin shell with viscoelastic core.
15. Y. C. Hu and S. C. Huang 1999 *Journal of Acoustical Society of America* **106**, 202–210. Forced response of sandwich ring with viscoelastic core subjected to traveling loads.
16. Y. C. Hu and S. C. Huang 1996 *Active Control of Vibration and Noise, American Society of Mechanical Engineers International Mechanical Engineering Congress and Exposition* **93**, 229–238. A linear theory of three-layer damped sandwich shell vibrations.
17. S. Mirza and A. V. Singh 1974 *American Institute of Aeronautics and Astronautics* **12**, 1418–1420. Axisymmetric vibration of circular sandwich plates.
18. P. K. Roy and N. Ganesan 1993 *Computers and Structures* **49**, 269–274. A vibration and damping analysis of circular plates with constrained damping layer treatment.
19. W. D. Iwan and K. J. Stahl 1973 *Journal of Mechanical Engineering*, *American Society of Mechanical Engineering* **40**, 445–451. The response of an elastic disk with a moving mass system.
20. S. G. Hutton, S. Chonan and B. F. Lehmann 1987 *Journal of Sound and Vibration* **112**, 527–539. Dynamic response of a guided circular saw.
21. I. Y. Shen and C. D. Mote Jr. 1991 *Journal of Sound and Vibration* **148**, 307–318. On the mechanisms of instability of circular plate under a rotating spring–mass–dashpot system.
22. I. Y. Shen 1993 *American Society of Mechanical Engineers Journal of Vibration and Acoustics* **115**, 65–69. Response of a stationary, damped, circular plate under a rotating slider bearing system.
23. S. C. Huang and B. S. Hsu 1992 *American Society of Mechanical Engineering Journal of Vibration and Acoustics* **114**, 468–476. Receptance theory applied to modal analysis of a spinning disk with interior multi-point supports.
24. W. Soedel 1993 *Vibrations of Shells and Plates,* New York: Marcel Dekker.
25. A. W. Leissa 1969 *Vibrations of Plates*. Washington, DC: US Government Printing Office.

APPENDIX A

$$\beta_r^i = -\frac{\partial u_z}{\partial r}, \quad \beta_\theta^i = -\frac{1}{r}\frac{\partial u_z}{\partial \theta}, \quad i = c, p. \tag{A1}$$

The membrane forces are defined as

$$N_{rr}^i = k^i\left[\frac{\partial u_r^i}{\partial r} + \mu^i\left(\frac{1}{r}\frac{\partial u_\theta^i}{\partial \theta} + \frac{u_r^i}{r}\right)\right], \quad N_{\theta\theta}^i = k^i\left[\left(\frac{1}{r}\frac{\partial u_\theta^i}{\partial \theta} + \frac{u_r^i}{r}\right) + \mu^i\frac{\partial u_r^i}{\partial r}\right],$$
$$N_{r\theta}^i = \frac{k^i(1-\mu^i)}{2}\left[r\frac{\partial}{\partial r}\left(\frac{u_\theta^i}{r}\right) + \frac{1}{r}\frac{\partial u_r^i}{\partial \theta}\right], \quad i = p, c. \tag{A2}$$

$$N_{rr}^v = \frac{E^v h^v}{1-\mu^{v2}}\left\{\frac{1}{2}\left[\left(\frac{\partial u_r^c}{\partial r} + \frac{h^c}{2}\frac{\partial^2 u_z}{\partial r^2}\right) + \left(\frac{\partial u_r^p}{\partial r} - \frac{h^p}{2}\frac{\partial^2 u_z}{\partial r^2}\right)\right] + \frac{\mu^v}{2r}\left[\left(\frac{\partial u_\theta^c}{\partial \theta}\right.\right.\right.$$
$$\left.\left.\left. + \frac{h^c}{2r}\frac{\partial^2 u_z}{\partial \theta^2}\right) + \left(\frac{\partial u_\theta^p}{\partial \theta} - \frac{h^p}{2r}\frac{\partial^2 u_z}{\partial \theta^2}\right) + \left(u_r^c + \frac{h^c}{2}\frac{\partial u_z}{\partial r}\right) + \left(u_r^p - \frac{h^p}{2}\frac{\partial u_z}{\partial r}\right)\right]\right\},$$

$$N^v_{\theta\theta} = \frac{E^v h^v}{1-\mu^{v2}}\left\{\frac{1}{2r}\left[\left(\frac{\partial u^c_\theta}{\partial\theta} + \frac{h^c}{2r}\frac{\partial^2 u_z}{\partial\theta^2}\right) + \left(\frac{\partial u^p_\theta}{\partial\theta} - \frac{h^p}{2r}\frac{\partial^2 u_z}{\partial\theta^2}\right) + \left(u^c_r + \frac{h^c}{2}\frac{\partial u_z}{\partial r}\right) + \left(u^p_r - \frac{h^p}{2}\frac{\partial u_z}{\partial r}\right)\right] + \frac{\mu^v}{2}\left[\left(\frac{\partial u^c_r}{\partial r} + \frac{h^c}{2}\frac{\partial^2 u_z}{\partial r^2}\right) + \left(\frac{\partial u^p_r}{\partial r} - \frac{h^p}{2}\frac{\partial^2 u_z}{\partial r^2}\right)\right]\right\}. \tag{A3}$$

The bending moments are defined as

$$M^i_{rr} = -D^i\left[\frac{\partial^2 u_z}{\partial r^2} + \mu^i\left(\frac{1}{r^2}\frac{\partial^2 u_z}{\partial\theta^2} + \frac{1}{r}\frac{\partial u_z}{\partial r}\right)\right],$$

$$M^i_{\theta\theta} = -D^i\left[\left(\frac{1}{r^2}\frac{\partial^2 u_z}{\partial\theta^2} + \frac{1}{r}\frac{\partial u_z}{\partial r}\right) + \mu^i\frac{\partial^2 u_z}{\partial r^2}\right], \quad i = p, c$$

$$M^i_{r\theta} = -\frac{D^i(1-\mu^i)}{2}\left[r\frac{\partial}{\partial r}\left(\frac{1}{r^2}\frac{\partial u_z}{\partial\theta}\right) + \frac{1}{r}\frac{\partial^2 u_z}{\partial r\partial\theta}\right], \tag{A4}$$

$$M^v_{rr} = \frac{E^v h^{v3}}{12(1-\mu^{v2})}\left\{\frac{h^c + h^p}{2h^v}\frac{\partial^2 u_z}{\partial r^2} + \mu^v\frac{h^c + h^p}{2rh^v}\left(\frac{1}{r}\frac{\partial^2 u_z}{\partial\theta^2} + \frac{\partial u_z}{\partial r}\right)\right\},$$

$$M^v_{\theta\theta} = \frac{E^v h^{v3}}{12(1-\mu^{v2})}\left\{\frac{h^c + h^p}{2rh^v}\left(\frac{1}{r}\frac{\partial^2 u_z}{\partial\theta^2} + \frac{\partial u_z}{\partial r}\right) + \mu^v\frac{h^c + h^p}{2h^v}\frac{\partial^2 u_z}{\partial r^2}\right\}. \tag{A5}$$

The shear force resultants of VEM are defined as

$$Q^v_{rz} = G^v h^v\left\{\frac{1}{h^v}\left[\left(u^c_r + \frac{h^c}{2}\frac{\partial u_z}{\partial r}\right) - \left(u^p_r - \frac{h^p}{2}\frac{\partial u_z}{\partial r}\right)\right] + \frac{\partial u_z}{\partial r}\right\},$$

$$Q^v_{\theta z} = G^v h^v\left\{\frac{1}{h^v}\left[\left(u^c_\theta + \frac{h^c}{2}\frac{1}{r}\frac{\partial u_z}{\partial\theta}\right) - \left(u^p_\theta - \frac{h^p}{2}\frac{1}{r}\frac{\partial u_z}{\partial\theta}\right)\right] + \frac{1}{r}\frac{\partial u_z}{\partial\theta}\right\}. \tag{A6}$$

The coefficients of $c_a, c_b, \ldots, c_n$ are defined as

$$A^i_1 = \frac{1+\mu^i}{2}, \quad A^i_2 = \frac{1-\mu^i}{2}, \quad A^i_3 = \frac{3-\mu^i}{2}, \quad i = p, c,$$

$$c_a = -3A^p_2 + A^c_2 - A^p_1 A^c_3 + 2A^c_1 A^p_2, \quad c_b = 3A^p_2 - A^c_2 - A^p_3 A^c_3 - 2A^c_1 A^p_3, \tag{A7}$$

$$c_c = 3A^p_3 - A^p_2 A^c_3 - 2A^c_1 A^p_2, \quad c_d = -3A^p_3 + A^p_2 A^c_3 + 2A^c_1 A^p_2,$$

$$c_e = -2 - A^p_2 A^c_3 + 2A^c_1 A^p_2, \quad c_f = A^p_2 + A^c_2 + A^c_1 A^p_1,$$

$$c_g = A^p_1 + A^c_1 A^p_2, \quad c_h = A^c_2 A^p_2,$$

$$c_i = A_2^c A_3^p - A_3^c - 2A_1^c, \quad c_j = A_1^c + A_1^p A_2^c,$$
$$c_k = 1 + k^p/k^c, \quad c_l = A_2^c + A_2^p k^p/k^c,$$
$$c_m = A_3^c + A_3^p k^p/k^c, \quad c_n = A_1^c + A_1^p k^p/k^c.$$

The coefficients of $d_a, d_b, \ldots, d_n$ are defined as

$$d_a = -2 - 2A_2^c A_2^p, \quad d_b = 2A_1^c - A_3^c + 3A_2^c A_3^p,$$
$$d_c = -A_1^c - A_1^p A_2^c, \quad d_d = -A_1^p - A_1^c A_2^p,$$
$$d_e = 2A_1^c A_2^p - A_3^p - A_2^p A_3^c, \quad d_f = 2A_1^c - A_2^p - A_2^p A_3^c + 3A_2^c,$$
$$d_g = -2A_2^c A_3^p + A_2^p + A_3^p A_3^c - 3A_2^c, \quad d_h = -A_2^p - A_1^p A_1^c - A_2^c,$$
$$d_i = A_2^p A_2^c, \quad d_j = 3A_2^p A_2^c,$$
$$d_k = A_1^c + A_1^p k^p/k^c, \quad d_l = A_3^c + A_3^p k^p/k^c,$$
$$d_m = 1 + k^p/k^c, \quad d_n = A_2^c + A_2^p k^p/k^c. \tag{A8}$$

$$m_n = (\rho^p h^p + \rho^c h^c + \rho^v h^v) \int_b^a R_n(r) R_n(r) r \, \mathrm{d}r. \tag{A9}$$

$$f_s(r) = \sin\frac{(r-b)\pi}{2l}, \quad f_c(r) = \cos\frac{(r-b)\pi}{2l}$$
$$k_{11} = \frac{k^p h^v}{G^v}\int_b^a (B_1 + B_4) f_s(r) r \, \mathrm{d}r, \quad k_{12} = \frac{k^p h^v}{G^v}\int_b^a (B_2 + B_5) f_s(r) r \, \mathrm{d}r,$$
$$k_{13} = \frac{h^p + h^c + 2h^v}{2}\int_b^a B_3 f_s(r) r \, \mathrm{d}r, \quad k_{21} = \frac{k^p h^v}{G^v}\int_b^a (B_6 + B_9) f_s(r) r \, \mathrm{d}r,$$
$$k_{22} = \frac{k^p h^v}{G^v}\int_b^a (B_7 + B_{10}) f_s(r) r \, \mathrm{d}r, \quad k_{23} = -\frac{h^p + h^c + 2h^v}{2}\int_b^a B_8 f_s(r) r \, \mathrm{d}r,$$
$$k_{31} = -\int_b^a B_{14} R_n(r) r \, \mathrm{d}r, \quad k_{32} = -\int_b^a B_{15} R_n(r) r \, \mathrm{d}r,$$
$$k_{33} = \int_b^a B_{16} R_n(r) r \, \mathrm{d}r. \tag{A10}$$

$$B_1 = [(3\pi^2 + c_d n^2 \pi^2)/4rl^2 + r\pi^4/16l^4 + (n^4 c_h - n^2 c_b - 3)/r^3] f_s(r)$$
$$\quad + [(3\pi - c_a n^2 \pi)/2r^2 l - \pi^3/4l^3] f_c(r),$$
$$B_2 = [(c_c n - c_j n^3)\pi/2lr^2 - c_g n\pi^3/8l^3] f_c(r) - c_e n\pi^2 f_s(r)/4rl^2 + (c_d n - c_i n^3) f_s(r)/r^3,$$
$$B_3 = P_n[2 - 2(1+n^2)(r-b)/r + 2n^2(r-b)^2/r^2] + Q_n[12r - 6b - (3+3n^2)(r-b)^2/r]$$
$$\quad + 2n^2(r-b)^3/r^2] + R_n[12(r-b)^2 + 24r(r-b) - (4+4n^2)(r-b)^3/r$$
$$\quad + 2n^2(r-b)^4/r^2],$$
$$B_4 = [-c_k\pi/2l] f_c(r) + [c_k r\pi^2/4l^2 + (c_k + c_l n^2)/r] f_s(r),$$
$$B_5 = (-c_n n\pi/2l) f_c(r) + (c_m n/r) f_s(r),$$

$$B_6 = [(d_b n - d_d n^3)\pi/2lr^2 - d_c n\pi^3/8l^3]f_c(r) - [d_a n\pi^2/4rl^2 + (d_b n + d_h n^3)/r^3]f_s(r),$$
$$B_7 = ((d_g n^2 + n^4 - d_j)/r^3 - r d_i \pi^4/16l^4 + [(d_j - d_h n^2)\pi^2/4rl^2])f_s(r)$$
$$+ ([(d_f n^2 + d_j)\pi/2lr^2] - 2d_i\pi^3/8l^3)f_c(r),$$

$$B_8 = nP_n[2 + 2(r-b)/r - n^2(r-b)^2/r^2] + nQ_n[6(r-b) + 3(r-b)^2/r$$
$$- n^2(r-b)^3/r^2] + nR_n[12(r-b)^2 + 4(r-b)^3/r - n^2(r-b)^4/r^2],$$

$$B_9 = (d_k n\pi/2l)f_c(r) + (d_l n/r)f_s(r),$$
$$B_{10} = -d_n[\pi/2l]f_c(r) + [(d_m n^2 + d_n)/r + d_n(\pi/2l)^2 r]f_s(r),$$
$$B_{11} = [(\pi/2l)(1+n^2)/r^2 + (\pi/2l)^3]f_c(r) + [\pi^2/2rl^2 + (n^2-1)/r^3]f_s(r),$$
$$B_{12} = [(n^3 - n)/r^3 + n\pi^2/4rl^2]f_s(r) + n\pi/2r^2 l f_c(r),$$
$$B_{13} = P_n[-2(1+2n^2)/r^2 + (2+4n^2)(r-b)/r^3 + (n^4 - 4n^2)(r-b)^2/r^4]$$
$$+ Q_n[12/r + (3+6n^2)(r-b)^2/r^3 - (6+12n^2)(r-b)/r^2$$
$$+ (n^4 - 4n^2)(r-b)^3/r^4] + R_n[24 + 48(r-b)/r + (4+8n^2)(r-b)^3/r^3$$
$$- (12+24n^2)(r-b)^2/r^2 + (n^4 - 4n^2)(r-b)^4/r^4],$$
$$B_{14} = k^p B_{11}(h^p + h^c + 2h^v)/2, \quad B_{15} = k^p B_{12}(h^p + h^c + 2h^v)/2, \quad B_{16} = (D^c + D^p)B_{13}. \quad \text{(A11)}$$

$$q_1 = \frac{1}{\alpha_n}\int_b^a\int_0^{2\pi} q_z^c \cos(n\theta) R_n(r) r \, dr \, d\theta, \alpha_n = \begin{cases} \pi, n \neq 0, \\ 2\pi, n = 0. \end{cases}$$
$$q_2 = \frac{1}{\beta_n}\int_b^a\int_0^{2\pi} q_z^c \sin(n\theta) R_n(r) r \, dr \, d\theta, \beta_n = \begin{cases} \pi, n \neq 0, \\ 0, n = 0. \end{cases} \quad \text{(A12)}$$

APPENDIX B: NOMENCLATURE

D^i	bending ridigity of layers, $i = p, v, c$
E^i	Young's modulus of layers, $i = p, c$
G^v	complex shear modulus of VEM
h^i	thickness of layers, $i = p, v, c$
$\mathbf{K}_n$	stiffness matrix of the discretized EOM's
k^i	bending strains, $i = p, c$
k_{jm}, k_n	elements of stiffness matrix $\mathbf{K}_n$, $j, m = 1-3$, equivalent stiffness
$\mathbf{M}_n$	mass matrix of the discretized EOM's
m, m_n	radial wave number, equivalent transverse mass
M^i_{jm}	bending moments of each layers, $j, m = r, \theta, i = p, v, c$
n	circumferential wave number
N^i_{jm}	membrane forces of each layer, $j, m = r, \theta, i = p, v, c$
$\mathbf{Q}_{an}, \mathbf{Q}_{bn}$	generalized force vectors
q_j	generalized force, $j = 1-3$
Q^i_{jz}	shear force resultants of each layer, $j = r, \theta, i = p, v, c$
r	co-ordinate in radial direction
$\mathbf{X}_{an}, \mathbf{X}_{bn}$	generalized co-ordinate vectors
t	time
u^i_j	displacements of middle surface of a layer, $j = r, \theta, z, i = p, v, c$
z	transverse co-ordinate

Greek letters

generalized co-ordinates	$\alpha_{mn}, \psi_{mn}, \varphi_{mn}, \phi_{mn}, \zeta_{mn}, \beta_{mn}$
β_j^i	rotational angle of layers, $j = r, \theta, i = p, v, c$
δ	Dirac delta function
ξ	damping ratio
θ	circumferential co-ordinate
ρ^i	density of layers, $i = p, v, c$
$\mathbf{\Omega}$	load's rotating speed
ω	driving frequency
μ^i	The Poisson ratio of layers, $i = p, v, c$

Superscripts

c	constraining layer
p	plate
v	viscoelastic core